Durairaj, Vasuki; Wester, Niklas; Etula, Jarkko; Laurila, Tomi; Lehtonen, Janika; Rojas, Orlando J.; Pahimanolis, Nikolaos; Koskinen, Jari

Multiwalled Carbon Nanotubes/Nanofibrillar Cellulose/Nafion Composite-Modified Tetrahedral Amorphous Carbon Electrodes for Selective Dopamine Detection

Published in:
Journal of Physical Chemistry C

DOI:
10.1021/acs.jpcc.9b05537

Published: 01/01/2019

Document Version
Peer reviewed version

Published under the following license:
Unspecified

Please cite the original version:
Durairaj, V., Wester, N., Etula, J., Laurila, T., Lehtonen, J., Rojas, O. J., Pahimanolis, N., & Koskinen, J. (2019). Multiwalled Carbon Nanotubes/Nanofibrillar Cellulose/Nafion Composite-Modified Tetrahedral Amorphous Carbon Electrodes for Selective Dopamine Detection. *Journal of Physical Chemistry C*, *123*(40), 2482624836 . https://doi.org/10.1021/acs.jpcc.9b05537

Multi-Walled Carbon Nanotubes/Nanofibrillar Cellulose/Nafion® Composite-Modified Tetrahedral Amorphous Carbon Electrodes for Selective Dopamine Detection

Vasuki Durairaj,[†] Niklas Wester,[†] Jarkko Etula,[†] Tomi Laurila,[‡] Janika Lehtonen,[§] Orlando J. Rojas,[§] Nikolaos Pahimanolis,[∥] and Jari Koskinen.[†]*

[†] Department of Chemistry and Materials Science, School of Chemical Technology, Aalto University, P.O. Box 16100, 00076 Aalto, Finland

[‡] Department of Electrical Engineering and Automation, School of Electrical Engineering, Aalto University, P.O. Box 13500, 00076 Aalto, Finland

[§] Department of Bioproducts and Biosystems, School of Chemical Technology, Aalto University, P.O. Box 16100, 00076 Aalto, Finland

[∥] Betulium Oy, Tekniikantie 2, FI-02150, Espoo, Finland

Corresponding Author

* Tel.: +358505138355. E-mail: vasuki.durairaj@aalto.fi (Vasuki Durairaj)

ABSTRACT: We introduce a composite membrane comprising of multi-walled carbon nanotubes (MWCNTs) dispersed in a matrix of sulfated nanofibrillar cellulose (SNFC) and Nafion. The high negative charge densities of the SNFC and Nafion ionomers enhance the cationic selectivity of the composite. The composite is characterized by scanning electron (SEM) and transmission electron (TEM) microscopies as well as Fourier transform infrared (FTIR) and Raman spectroscopies. Tetrahedral amorphous carbon (ta-C) electrodes modified with the composite are investigated as potential dopamine (DA) electrochemical sensors. The composite-modified electrodes show significant selectivity and sensitivity towards DA in the presence of ascorbic acid (AA) and uric acid (UA) in physiologically relevant concentrations. A linear dopamine detection range of 0.05 – 100 μM with detection limits of 65 nM in PBS and 107 nM in interferent solution was determined using 100 mV/s cyclic voltammetry (CV) measurements. These results highlight the potential of the composite membrane for *in vivo* detection of neurotransmitters.

---

1. INTRODUCTION

Tetrahedral amorphous carbon (ta-C) thin films are highly versatile coatings made using a low-cost, patternable, and complementary metal−oxide−semiconductor (CMOS) compatible room temperature deposition process[1] and are chemically inert.[2] Their biocompatibility and resistance to fouling,[3,4] combined with a wide potential window,[5–8] makes them an attractive electrode material for *in vivo* electrochemical sensing of biomolecules. However, a major drawback of the ta-C electrodes is the lack of selectivity between various analytes. Various surface functionalizations,[7,9] doping,[6,8,10] and thin film modifications[11–14] of the ta-C electrode are typically employed to improve the selectivity towards different analytes. In particular, modifications with high surface area carbon nanomaterials[15,16] have been shown to significantly enhance the electrocatalytic properties of the ta-C electrode[11–13] for detection of biomolecules such as dopamine (DA).

Dopamine is a neurotransmitter that plays a vital role in the cognitive and motor control functions of the brain. Local *in vivo* concentrations of dopamine in brain vary between 10 nM (overall basal level) to 1 µM (at the time of release events).[17] Sensitive and selective detection of dopamine requires that the electrode is able to detect nanomolar levels of dopamine in the presence of interferents like uric acid (UA) and ascorbic acid (AA) which are typically present in concentrations of around 500 µM and 1 mM, respectively. Several studies are reported on sensitive detection of dopamine using various electrode materials.[18–21] Improved selectivity is often achieved using thin films or composites of permselective polymers like Nafion[22–24] and various functionalized carbon nanomaterials.[11,13,15,25] However, to the best of the authors' knowledge, none of these studies have demonstrated both selectivity and sensitivity towards nanomolar levels of dopamine in the presence of physiologically relevant concentrations of anionic interferents in cyclic voltammetry measurements.

Integrating high surface area functional nanomaterials in a hygroscopic matrix such as nanocellulose can significantly improve the wetting and consequently the response time of a hybrid electrode material. Nanofibrillar cellulose (NFC), obtained from plant cellulose, has proven to be a promising material for engineered biopolymer membranes and composites in numerous applications including filtration, biomimetic membranes, drug delivery, energy storage and sensing.[26] The fibrils are extracted from the hemicellulose and lignin matrix of wood pulp by a combination of mechanical treatments such as grinding and homogenization along with chemical pre-treatments to loosen the rigid cellulose structure.[27] They comprise both crystalline and amorphous regions of cellulosic molecules, with dimensions in the order of few nanometers in diameter and up to several micrometers in length.[28] Reconstituted nanocellulose and nanocellulose/polymer composite membranes have attracted tremendous research interest in various applications including electrochemical sensing.[29–31] Chemical pre-treatment of the cellulose nanofibrils enable the introduction of charged (anionic) functional

groups such as carboxylic, sulfate, sulfonic or phosphoric groups on the NFCs. Such charged NFCs have a high negative ζ–potential and hence form stable colloidal suspensions which have been used to effectively disperse nanomaterials for fabrication of functional composites.[32–34]

There has been increasing interest in nanocellulose and carbon nanomaterial composites in the recent years, especially in energy storage applications[35,36] and transparent electronics,[32,37] owing to the highly attractive properties of both these materials, which are often enhanced favorably in the composites. Investigation of such composites for electrochemical sensing applications are however still limited.[38–40] In this study, we propose a composite membrane with multi-walled carbon nanotubes (MWCNTs) integrated in a highly sulfated nanofibrillar cellulose (SNFC) and Nafion® matrix, for electrochemical detection of dopamine. Introducing high surface charge densities in the matrix, using functionalized nanocellulose and Nafion ionomers, allows for tailoring of the ion flux in the matrix as well as stable dispersion of MWCNTs. An improved selectivity towards cationic DA is observed, due to the combined effect of the anionic sulfonic groups in Nafion and sulfate groups in the nanocellulose. Nafion further serves as a binder to keep the hydrophilic cellulose matrix adhered to the hydrophobic ta-C electrode.

2. EXPERIMENTAL SECTION

2.1. Composite preparation. Multi-walled carbon nanotubes grown by chemical vapor deposition (CVD) process (purity > 95%) were purchased from NanoLab, Inc. (Newton, MA). The MWCNTs are specified to have outer diameter in the range of 30±15 nm and 5–20 μm length. The MWCNTs were used as-received in the composite, without pre-treatments. Water suspensions (1.5 wt%) of highly sulfated nanofibrillar cellulose (SNFC), 5–10 nm diameter and ~200 nm long, were kindly provided by Betulium Oy. The degree of sulfation as specified by the manufacturer is 1.8 mmol/g (or average degree of substitution, DS = 0.36). Nafion® D-521 (molecular weight 544.135 g/mol) 5 wt% dispersion was purchased from Alfa Aesar.

The composite mixture was prepared by dispersing 0.11 g MWCNTs in 12 g of 0.375 wt % SNFC and 2 g of 5 wt % Nafion and diluting the mixture with 5.9 g of ethanol (> 99.5 %). The final dry weight percentages of MWCNTs, SNFC and Nafion in the mixture were 0.55, 0.225 and 0.49 %, respectively (MWCNTs : SNFC : Nafion = 2.4 : 1 : 2.2). The ratio of SNFC to MWCNTs was chosen to be ~ 1 : 2, as higher ratios of SNFCs resulted in suspensions too thick to be drop-casted and lower ratios resulted in inhomogeneous suspensions. The weight percentage of Nafion was chosen to be equal to that of MWCNTs to facilitate homogeneous functionalization of the MWCNTs by Nafion ionomers and ensure good binding of the composite to the hydrophobic electrode surface. After magnetically stirring for 48 hours and ultra-sonication for 30 minutes a stable suspension was achieved. As a control test, mixtures of MWCNT/SNFC (2.4 : 1) and MWCNT/Nafion (2.4 : 2.2) with same weight percentages were also prepared in a similar manner. The suspensions were stored in the refrigerator and prior to drop casting on ta-C electrodes, the solutions were ultra-sonicated for 5 minutes.

2.2. Electrode fabrication. The ta-C thin film electrodes were prepared by filtered cathodic vacuum arc (FCVA) deposition on highly conductive, p-type, boron-doped <100> Si wafers with < 0.005 Ohm- cm resistivity (Siegert Wafer, Germany). Before deposition of a 7 nm ta-C layer, a 20 nm Ti adhesion layer was deposited by means of direct current magnetron sputtering. The fabrication and characterization of ta-C electrodes are discussed in detail in previous work.[8] The ta-C coated wafer was diced with an automated dicing saw (DAD 3220, Disco) into 5 mm x 5 mm pieces. The pieces were then packaged onto copper-clad FR4-PBB sheets with a 3 mm circular exposed area (0.07 cm^2 effective electrode area) using a PTFE film (Saint-Gobain Performance Plastics CHR 2255-2). 5 µL drops of the MWCNT/SNFC/Nafion ternary composite as well as the control mixtures of MWCNT/SNFC and MWCNT/Nafion were drop-cast on the exposed surface of packaged ta-C electrodes and dried at room temperature for a minimum of 72 h prior to the electrochemical measurements. The

MWCNT/SNFC membranes dried in patches on the hydrophobic ta-C surface and delaminated rapidly in the electrolyte solution while the MWCNT/Nafion films contained non uniform clusters of MWCNTs in the Nafion matrix (Supplementary Figure S1). The electrochemical response of MWCNT/SNFC and MWCNT/Nafion modified ta-C electrodes were characterized in a solution containing 50 µM dopamine, 0.5 mM uric acid and 1 mM ascorbic acid. The MWCNT/SNFC modified electrodes were unstable due to delamination and the MWCNT/Nafion modified electrodes showed lower selectivity towards dopamine (Supplementary Figure S2). Therefore only the proposed composite of MWCNT/SNFC/Nafion was further characterized in the rest of this work.

2.3. Characterization. Fourier transform infrared spectroscopy (FTIR) was carried out using Bruker Alpha II FTIR spectrometer in attenuated total reflection (ATR) mode. The ATR-FTIR samples were prepared by drop-casting the composite and suspensions of individual materials on aluminum foil and drying at room temperature. Visible-Raman spectroscopy was performed on a Horiba Jobin-Yvon Labram HR confocal Raman system with 514 nm argon (Ar) laser. Spot size of 1 µm was used with an Olympus 100x objective. Spectroscopic calibration was performed on p-type silicon (Si) wafers (Ultrasil). The planar and cross-sectional morphology of the drop-cast composite membrane (5 µl in a 3 mm hole on Teflon taped Si wafer) was assessed using Hitachi S-4700 scanning electron microscope. The Teflon tape was removed before imaging and both planar and cross-sectional samples were coated with ~5 nm gold-palladium (Au-Pd) conductive layer by sputtering, for imaging. Non-coated samples prepared on ta-C chips were analyzed with energy dispersive X-ray spectroscopy (EDS) at low magnification using Tescan MIRA3 scanning electron microscope. High resolution transmission electron microscope (TEM) images were obtained using FEI Tecnai F20 at 200 kV acceleration voltage. TEM samples were prepared by drop casting a highly dilute (1:1000 in ethanol 99.5 %) solution of the composite on holey carbon copper grids (Agar Scientific).

The grids were dried at 70°C on a hot plate prior to imaging. ζ–potentials of a 0.025 wt % suspension of SNFCs in 1 mM KCl at pH 3, 5, 7, 9, and 11 were determined with Zetasizer Nano-ZS90 (Malvern).

2.4. Electrochemistry. Electrochemical properties of the composite-modified ta-C electrodes were assessed by cyclic voltammetry measurements using a Gamry Reference 600 potentiostat. A conventional three-electrode setup with an Ag/AgCl reference electrode (+ 0.199 V vs SHE, Radiometer Analytical) and a platinum wire counter was used. Conventional outer sphere redox probes $Ru(NH_3)_6Cl_3$ (hexaammineruthenium (III) chloride, Sigma-Aldrich), and K_2IrCl_6 (potassium hexachloroiridate (IV), Sigma-Aldrich) dissolved in 1 M KCl (Sigma-Aldrich) were used to characterize the charge selectivity. L-ascorbic acid, uric acid and dopamine hydrochloride were purchased from Sigma-Aldrich. CV measurements of dopamine were carried out both in phosphate buffer solution (PBS, pH = 7.4), and in a physiologically relevant interferent solution containing 1 mM AA and 0.5 mM UA dissolved in PBS. Electrodes were immersed in PBS solution 15 minutes prior to the measurements and were kept immersed for the duration of the measurements. The electrochemical cell was kept at nitrogen overpressure during measurements and all the measurements were carried out at room temperature.

3. RESULTS AND DISCUSSION

3.1. Physical properties: *3.1.1. Electron microscopy.* Planar scanning electron micrograph of the composite (Figure 1A) shows a dense fibrous surface over the entire area. The cross-sectional micrograph (Figures 1B) shows a network of fibers with varying thickness and morphology likely due to the presence of both MWCNTs and NFCs, which appear well dispersed. This is further observed in TEM images (Figures 1C, D), where similar fibrous structures are found, coated by Nafion. The larger MWCNT (> 15 nm diameter), with well-defined graphitic planes (lattice spacing 0.35 nm) and hollow cores, can be seen (Figure 1D)

interspersed with thinner (< 10 nm) nanocellulose fibers which show both amorphous and crystalline regions. EDS analysis (Supplementary Figure S3) of the composite film deposited on a ta-C coated silicon substrate shows the molybdenum (Mo) and iron (Fe) metal impurities from the MWCNTs dispersed throughout the composite membrane.

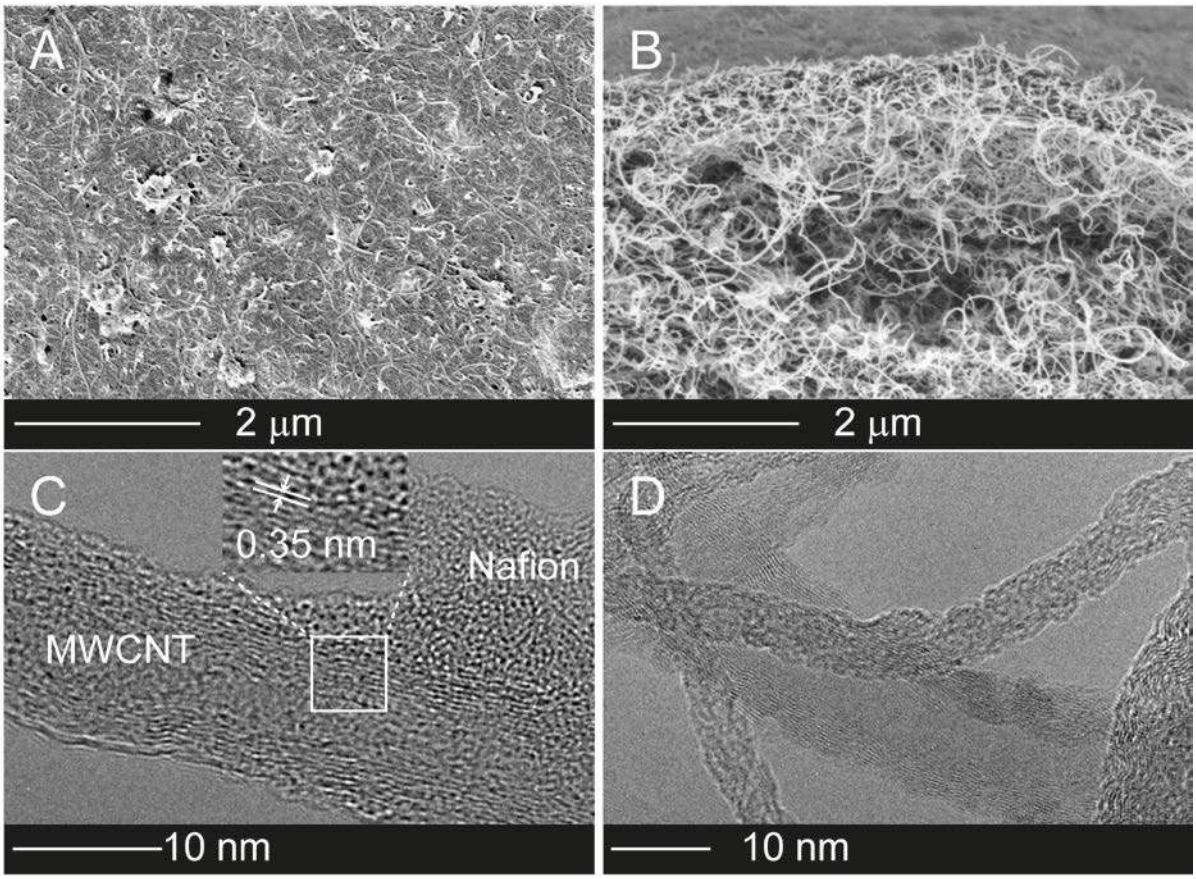

Figure 1. Planar (A) and cross-sectional (B) SEM images of the composite on Si-wafer; High resolution TEM images (C and D) of the composite. Inset in Figure C shows the graphitic lattice spacing on MWCNT wall.

3.1.2. ATR-FTIR. The absorbance spectra of SNFC (Betulium) together with that of unmodified nanofibrillar cellulose (from Department of Bioproducts and Biosystems, Aalto University) is shown in Figure 2A. Both samples were drop-casted on aluminum foils from aqueous suspensions and dried at ambient conditions for 24 hours prior to measurements. The SNFC shows strong peaks corresponding to the sulfate group, namely the symmetric C-O-S

vibration and assymetric S=O vibration, at around 810 and 1250 cm^{-1}, respectively.[41] In addition, a strong peak around 620 cm^{-1} can be observed, likely due to inorganic sulfate impurities from the sulfation process. These peaks are entirely absent in the unmodified NFC sample. The absorbance spectra of Nafion, MWCNTs and composite are shown together in Figure 2B, vertically offset for clarity. Suspensions of 5 wt % Nafion, MWCNTs in ethanol and composite mixture were also individually drop-cast on aluminum foils and allowed to dry at ambient conditions for 24 hours prior to measurement. The Nafion spectrum shows the characteristic CF_2 peaks at 512, 625, 1145 and 1200 cm^{-1} in addition to the sulfonic group peaks.[42] The composite membrane shows a large absorbance over the entire measurement window (400 to 4000 cm^{-1}), similar to that of the MWCNTs. However, in the sulfonic group fingerprint region (800 to 1600 cm^{-1} in Figure 2B), the composite shows distinct peaks indicating the functionalization of the MWCNTs by the Nafion and nanocellulose in the composite.

3.1.3. Raman spectroscopy. Raman spectra of the individual components as well as the composite, obtained with 514 nm argon laser are shown in Figures 2C and D. The Raman spectrum of p-type Si wafer, used as the substrate in all the Raman measurements, is shown in Figure 2C, along with Nafion and SNFC spectra, in the 50 to 3000 cm^{-1} region (vertically offset for clarity). Nafion spectrum shows strong peaks at 735, 804, 975, 1060, 1299 and 1374 cm^{-1}. The corresponding characteristic Nafion peak associations[43] are indicated in the figure. Characteristic cellulose peaks corresponding to C-O-C asymmetric (1096 cm^{-1}) and symmetric stretching (1122 cm^{-1}) and C-C ring asymmetric stretching (1160 cm^{-1}) of the β-1,4 – glycosidic cellulose unit are observed in the SNFC spectrum.[44] In addition, a distinct peak at 1060 cm^{-1} is also observed, which can be associated with the symmetric stretching of the sulfone $\nu_s(SO_3^-)$ from the sulfate functional group. The composite material (Figure 2D) primarily shows the intense Raman active D (1344 cm^{-1}) and G (1576 cm^{-1}) bands, as well as the 2D (2689 cm^{-1})

and E_{2g}+D (2927 cm^{-1}) bands arising from the MWCNTs.[45] No Nafion or nanocellulose contributions could be discerned relative to the Raman signal from the CNTs. No significant differences in the D and G band positions were observed in the composite compared to that of the individual MWCNTs, indicating that the MWCNTs were mostly unchanged structurally in the composite.

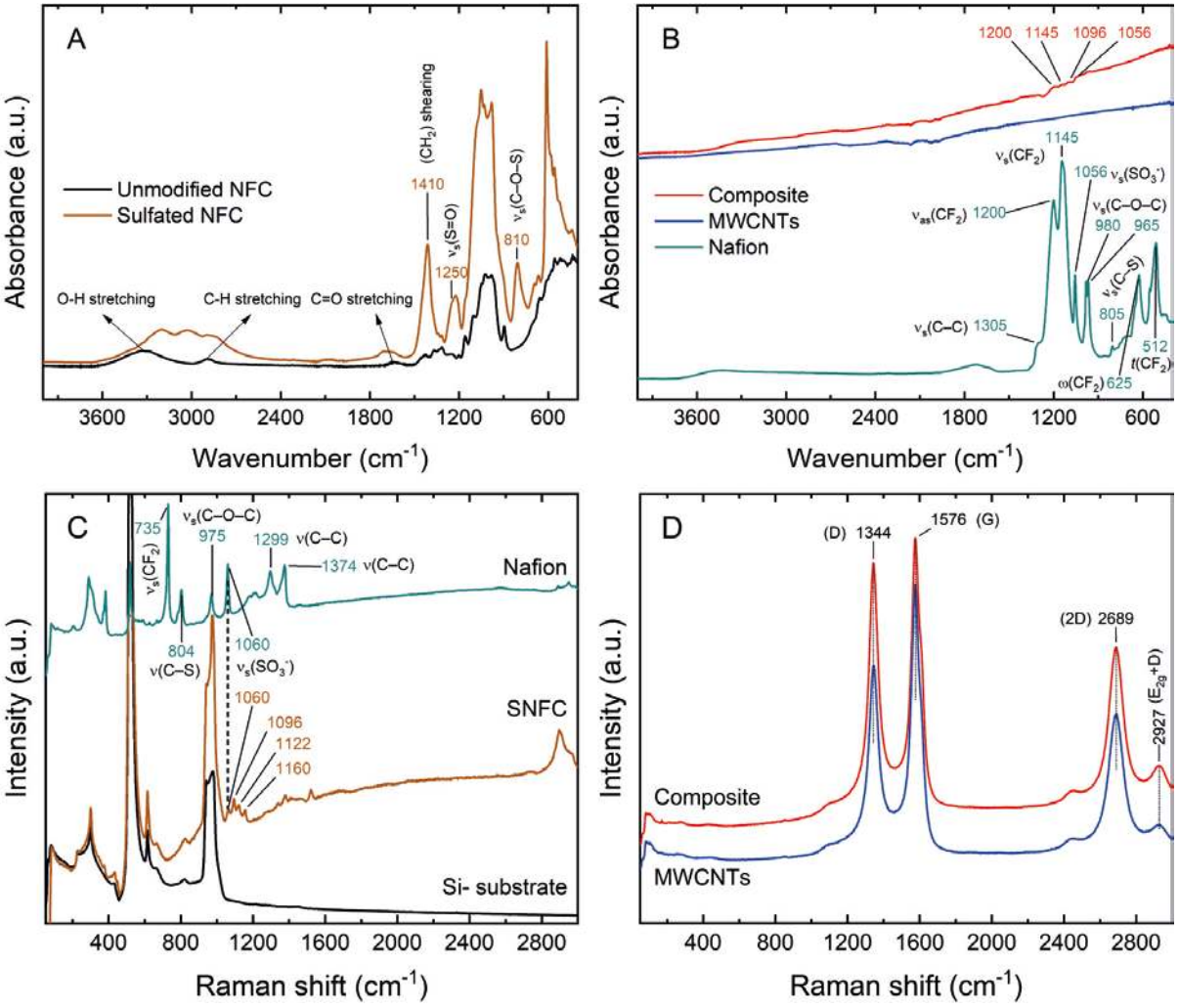

Figure 2. ATR-FTIR spectrum of (A) sulfated nanofibrillar cellulose and unmodified nanofibrillar cellulose reference, and (B) Nafion, MWCNTs and composite membrane. Raman spectra (C & D) of the composite membrane and individual materials on p-type Si substrate measured using 514 nm laser wavelength.

3.1.4. ζ–potential. The ζ–potential measurements were carried out with 0.025 wt% SNFC suspension in 1 mM KCl solution. The values were found to be ~ -27, -40, -40, -50 and -48 mV in pH 3, 5, 7, 9 and 11, respectively, indicating colloidally stable suspensions over a wide range of pH.

3.2. Electrochemical behavior. *In vivo* detection of dopamine transients requires high temporal resolution which can be achieved with fast scan CV measurements. Although higher sensitivity and selectivity can be obtained by differential pulse voltammetry (DPV) and slow scan rate (< 50 mV/s) CVs, all CV measurements in this work have been made at a scan rate of 100 mV/s to obtain results that are more relevant for *in vivo* measurements. All CV curves presented in this work are as measured and have not been smoothed or background subtracted. The peak currents are estimated with baseline subtraction for the scan rate studies but for the concentration studies and amperometry measurements the peak current values are taken from as measured CVs.

3.2.1. Charge selectivity. In order to investigate the selectivity of the composite membrane towards anionic and cationic molecules based on electrostatic effects, 1 mM solutions of standard outer sphere redox probes, namely positively charged $Ru(NH_3)_6Cl_3$ and negatively charged K_2IrCl_6 in 1 M KCl were used. The CVs of composite-modified ta-C electrode at 500 mV/s in 1 mM K_2IrCl_6 and 1 mM $Ru(NH_3)_6Cl_3$ solutions are shown in Figure 3A. The composite shows around 7 times higher sensitivity towards the cationic $Ru(NH_3)_6^{+2/+3}$ probe (I_{pa} = 235 µA at 500 mV/s CV) compared to the same concentration of anionic $IrCl_6^{-2/-3}$ probe (I_{pa} = 33 µA at 500 mV/s CV). Four different electrodes were measure at varying scan rates, from 25 to 1000 mV/s, in 1 mM K_2IrCl_6 as well as 1 mM and 5 mM $Ru(NH_3)_6Cl_3$ solutions. The linearization of background subtracted anodic (I_{pa}) and cathodic (I_{pc}) peak currents along with error bars are shown in Figures 3B, C and D, respectively. The anionic K_2IrCl_6 shows a linear relationship with square root of scan rate, indicating diffusion controlled behavior. At 1

mM concentration, the cationic $Ru(NH_3)_6Cl_3$ follows the direct scan rate, indicating electrostatic adsorption in the anionic cellulose matrix, as observed also by Thielemans et al.[46] However with higher concentration (5 mM) in the bulk solution, a diffusion controlled behavior is observed.

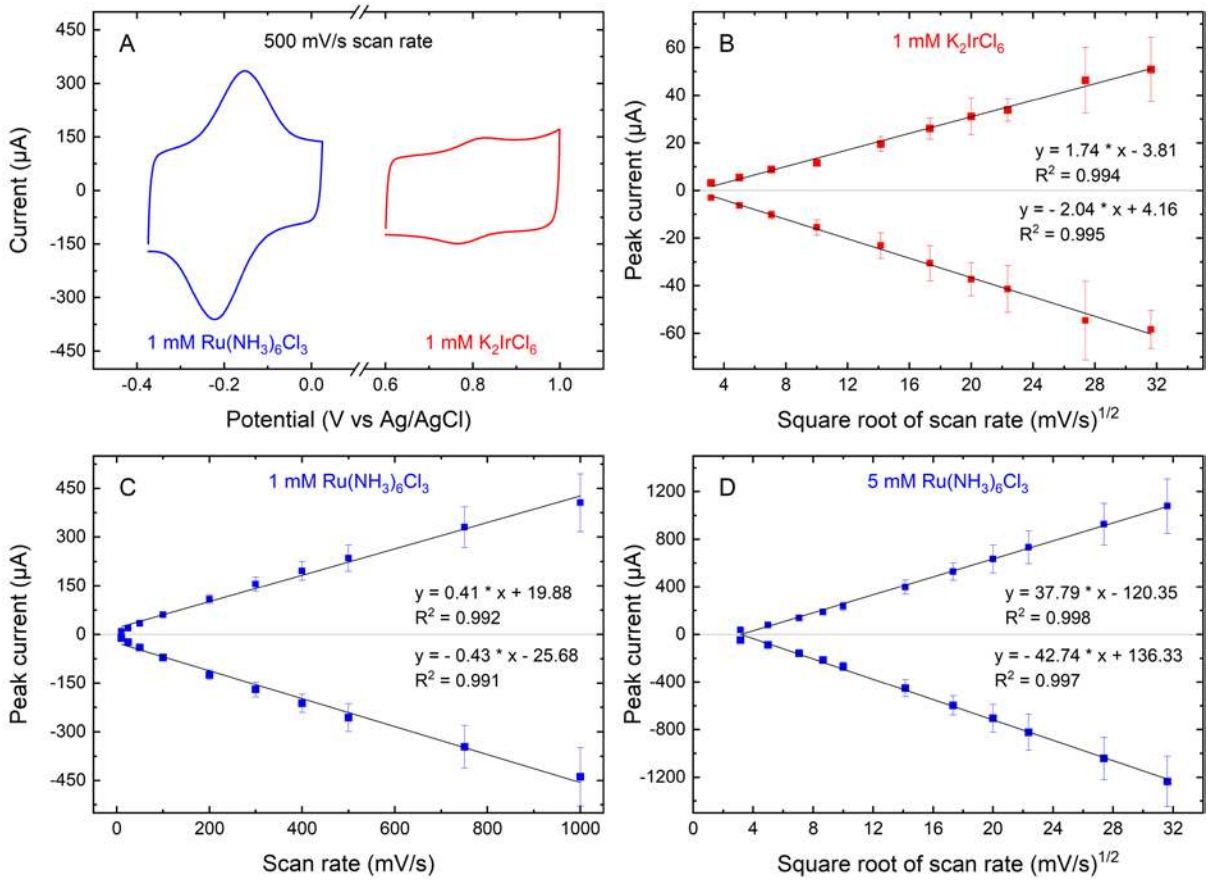

Figure 3. Cyclic voltammograms of composite-modified ta-C at 500 mV/s in 1 mM $Ru(NH_3)_6Cl_3$ and 1 mM K_2IrCl_6 solutions in 1 M KCl (A). The linearization curves of the redox currents of 1 mM K_2IrCl_6 versus square root of scanrate (B), 1 mM $Ru(NH_3)_6Cl_3$ versus direct scan rate (C) and 5 mM $Ru(NH_3)_6Cl_3$ versus square root of scanrate (D).

3.2.2. Adsorption of cationic molecules in the composite. The adsorption and enrichment of cationic molecules in the composite membrane was further investigated with washout tests for both outer sphere redox probe $Ru(NH_3)_6^{+2/+3}$ and the inner sphere cationic analyte dopamine (Figure 4) at a scan rate of 100 mV/s. A composite-modified electrode was cycled for

10 minutes in 1 mM $Ru(NH_3)_6Cl_3$ in 1 M KCl solution, followed by 7 minutes of washout in 1 M KCl solution. After the washout the electrode was remeasured in blank 1 M KCl solution. The oxidation peak of $Ru(NH_3)_6^{+2/+3}$ was negligible in the first cycle after washout, whereas a relatively low reduction peak was observed. After 10 cycles, the reduction peak was also significantly reduced and the CV followed that of the background in 1 M KCl (Figure 4A). The DA washout test was carried out by cycling a composite-modified electrode in 100 µM dopamine for 10 minutes, followed by 7 minutes washout in PBS and then remeasuring the electrode in PBS. Contrary to $Ru(NH_3)_6^{+2/+3}$ a strong signal of DA was observed, close to the intensity of the initial 100 µM DA solution signal, even after 7 minutes of washout in PBS. With further cycling the DA signal decreased gradually in intensity, but did not completely disappear even after 10 cycles (Figure 4B). These results indicate that while $Ru(NH_3)_6^{+2/+3}$ is likely only electrostatically adsorbed inside the composite matrix, the dopamine molecules are more strongly bound due to possible specific chemical interactions. To estimate the time response of the composite membrane to dopamine injections in physiologically relevant levels, amperometric measurements were carried out.

3.2.3. Amperometric response. The chronoamperometric response of the composite-modified ta-C electrode to dopamine addition in PBS was measured at a working potential of 290 mV (vs. Ag/AgCl) under constant stirring. Figure 4C shows the amperometric response from 1 µM to 100 µM dopamine injection over a time span of 500 seconds. A well-defined oxidation current can be observed already at 1 µM DA injection (inset of Figure 4C) with Savitzky-Golay smoothing. The electrode shows a fast time response of less than 1 second for the dopamine injections and a steady state current is observed in less than 5 seconds. The corresponding steady state current versus dopamine concentration curve is shown in Figure 4D, where a linear behavior is observed over the range of 1 to 100 µM DA concentration.

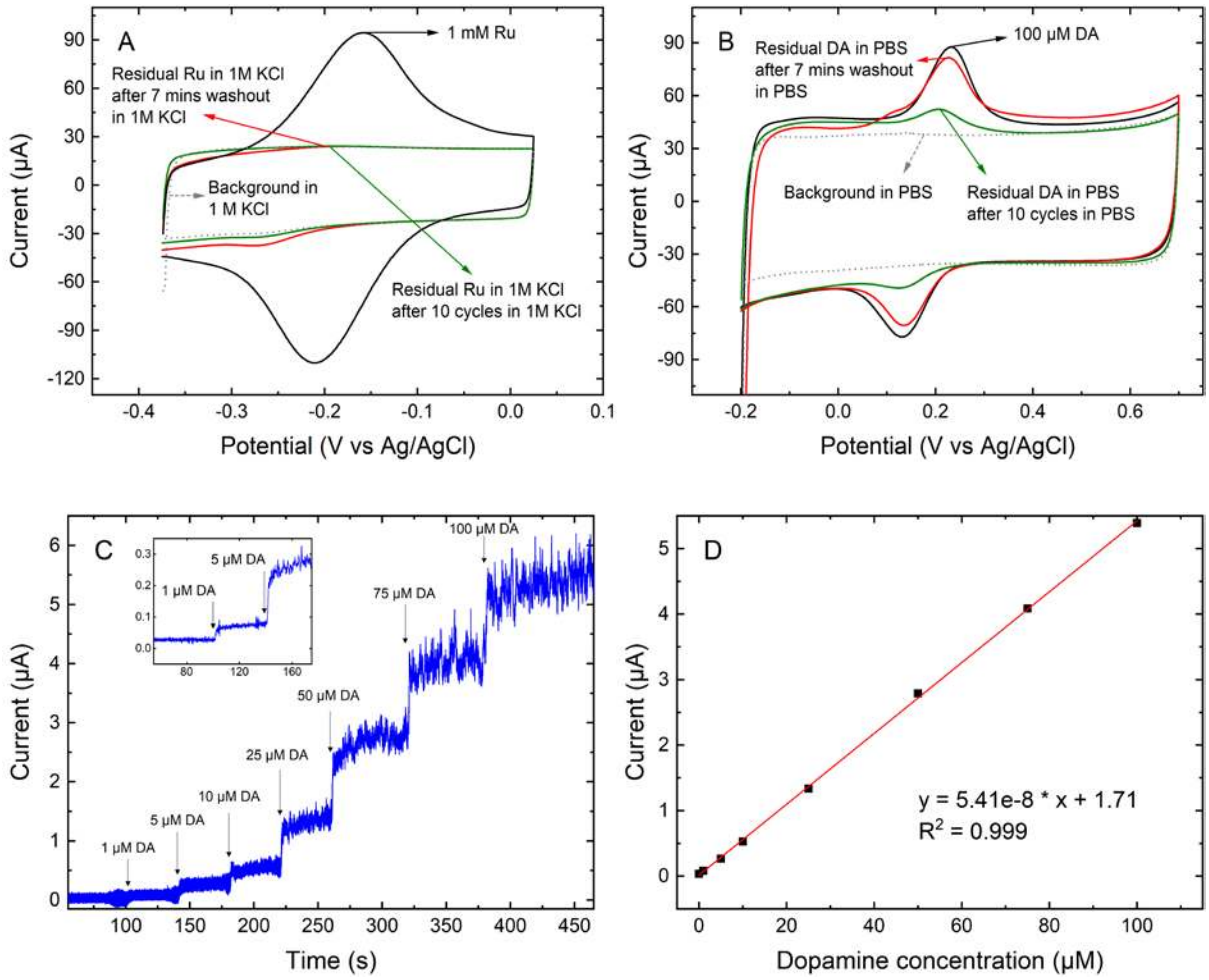

Figure 4. Cyclic voltammograms before and after washout of 1 mM $Ru(NH3)_6Cl_3$ in 1 M KCl (A) and 100 µM DA in PBS (B) from compositemodified ta-C electrodes at a scan rate of 100 mV/s. Amperometric response of the composite-modified ta-C electrode to dopamine injection in PBS under stirring, with the inset showing the smoothed data for 1 and 5 µM injections (C) and the corresponding current calibration (D).

3.2.4. Selectivity between DA, AA and UA. Figure 5A shows the cyclic voltammograms of unmodified ta-C electrode (black) and the composite-modified ta-C electrode (red), in a ternary interferent solution, containing 50 µM DA along with 1 mM AA and 0.5 mM UA, at a scan rate of 100 mV/s. The unmodified ta-C electrode is unable to resolve between the different analytes and shows an overlapping CV response. The composite-modified ta-C electrode

however, shows a clear distinction between the oxidation potentials of the different analytes, with significantly improved selectivity.

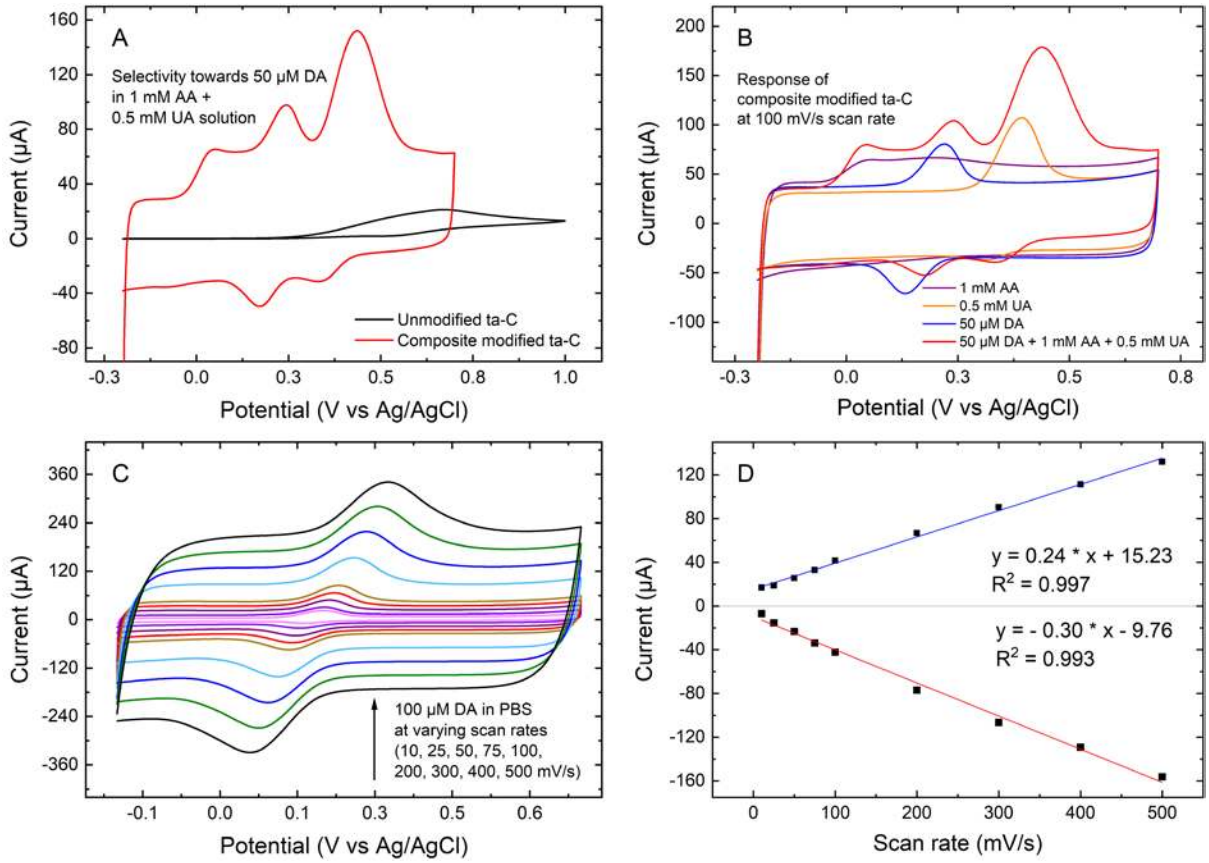

Figure 5. CVs of unmodified ta-C vs. composite-modified ta-C at 100 mV/s scan rate in interferent solution (A) and the response of the composite-modified ta-C at 100 mV/s scan rate to AA, UA and DA individually and in same solution (B). CVs of composite-modified ta-C at varying scan rates in 100 µM DA solution (C) and the linearization curve of anodic and cathodic peak currents of DA versus direct scan rate (D).

Compared to the unmodified ta-C electrode, all analytes exhibit a shift in the cathodic direction on the composite-modified electrode (Figure 5A), with AA exhibiting the largest shift. Despite the electrocatalytic effect, the AA peak intensity is found to be highly suppressed in comparison to previously reported values in materials functionalized with large surface area MWCNTs.[11,13] This suppression of AA and UA peak intensity in the composite is likely attributed to the large negative charge of the SNFCs as indicated by the ζ-potential

measurements, as well as the negative sulfonic functional groups in Nafion. The response of the composite-modified ta-C to the individual analytes (1 mM AA, 0.5 mM UA and 50 µM DA) in PBS are shown in Figure 5B along with the ternary interferent solution. Both DA and UA oxidation peaks can be clearly distinguished despite the broad tail of AA oxidation peak. The electrochemical response of dopamine on unmodified ta-C electrodes has been discussed in detail in earlier works.[13,47] Compared to the unmodified ta-C, the oxidation current of 100 µM DA in PBS increased by a factor of 30 for the composite-modified ta-C electrode.

3.2.5. Effect of scan rates. Figure 5C shows the cyclic voltammograms of the composite-modified ta-C electrode, obtained at varying scan rates (10 to 500 mV/s), in a PBS solution with 100 µM DA. The linear curves of anodic (I_{pa}) and cathodic (I_{pc}) peak currents of dopamine (Figure 5D) are directly proportional to scan rate, indicating adsorption of DA in the composite membrane, as observed also in the washout test. Both UA and AA show a diffusion controlled behavior, with the redox currents exhibiting a linear relationship with the square root of scan rate (supplementary Figure S4 & S5).

3.2.6. Sensitivity towards dopamine. The dopamine concentration measurements were carried out both in PBS and AA+UA interferent solutions by injecting aliquots of dopamine from stock solutions, while keeping the electrodes in the cell during the entire measurement series. Prior to DA injections, the electrodes were cycled in either the PBS or AA+UA starting solutions for 15 measurements of 1 cycle each, at 100 mV/s, to obtain a stable background. The last 3 measurements were used to estimate the standard deviation in background current (σ) for calculating the limit of detection. After each dopamine injection, the cell was bubbled with nitrogen for 5 seconds, followed by a single cycle CV measurement at 100 mV/s. Figures 6A and B show the response of the composite-modified ta-C electrode to varying concentrations of DA in PBS and interferent solutions, respectively. The measurements were repeated with three different electrodes in each case, to assess repeatability. A slight

background variation from electrode to electrode was observed, likely due to the variations in the drop-casting procedure. The calibration curves shown in Figure 6C and D include also the electrode to electrode variation, without any background corrections.

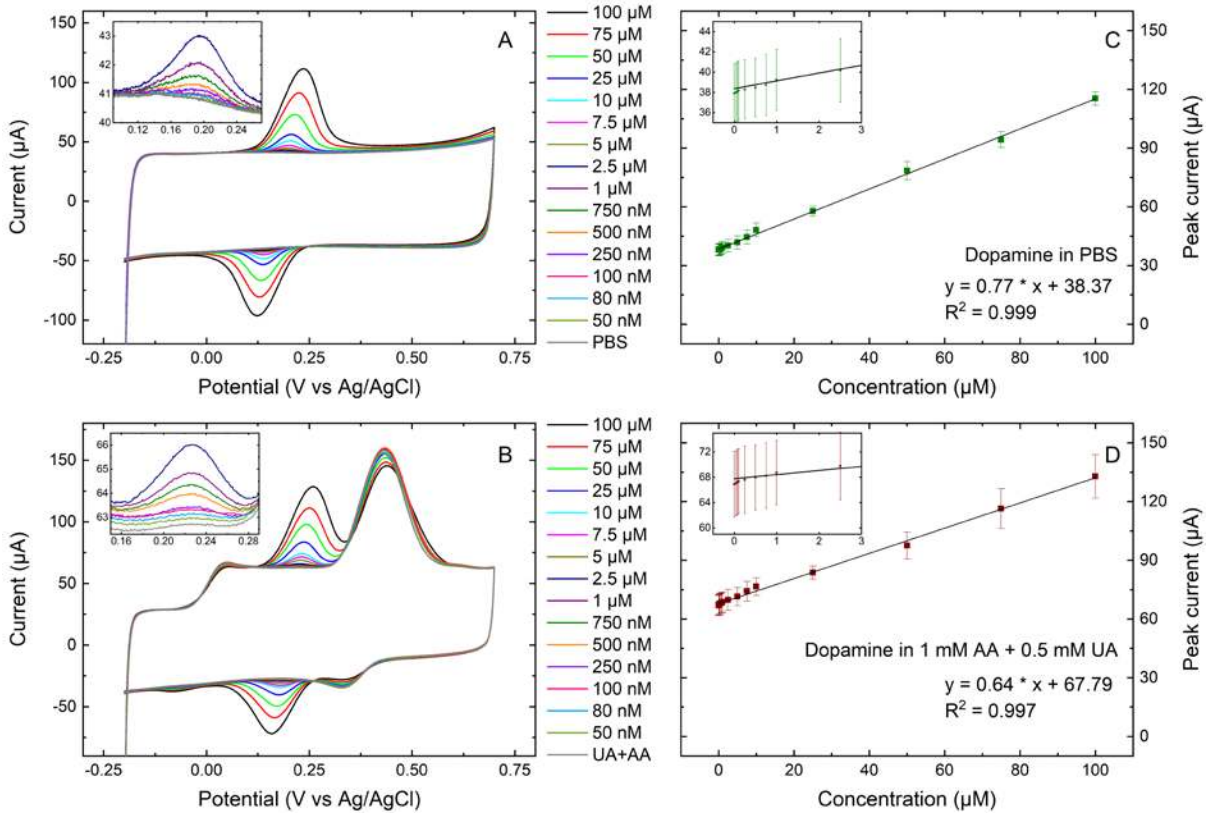

Figure 6. Cyclic voltammograms of composite-modified ta-C at 100 mV/s scan rate, showing the sensitivity towards dopamine at varying concentrations in (A) PBS solution and (B) 1 mM AA and 0.5 mM UA solution, with insets showing 0 to 2.5 µM DA concentrations. The corresponding current vs. concentration calibration curves with standard deviation (N=3) are shown in (C) and (D), with insets showing 0 to 2.5 µM DA concentrations.

The linear current vs. concentration relationships, in the range of 0.05 - 100 µM, in PBS and interferent solutions were I_{DA} (µA) = 0.77 * C_{DA} (µM) + 38.37 (R^2 = 0.999) and I_{DA} (µA) = 0.64 * C_{DA} (µM) + 67.79 (R^2 = 0.997), respectively. A reduction in the slope of DA peak current vs. concentration by 16.17% was observed in the interferent solution. Despite this decrease in sensitivity, a distinct peak of DA oxidation can still be seen for 500 nM DA (inset

of Figure 6B), which corresponds to the dopamine levels expected at the time of release events in brain. The sensitivity of the composite-modified ta-C electrode towards DA with varying concentrations of AA was further investigated by keeping the DA concentration constant at 1 µM and varying the AA concentrations from 0.1 to 1.5 mM. The results are presented in Figure 7, together with the corresponding DA current vs AA concentration calibration. A clear peak for 1 µM DA can be observed at all AA concentrations in Figure 7A. The DA peak currents plotted in Figure 7B are as observed in the CV scan, without subtracting the AA interference, and they follow a linear relationship with respect to the AA concentration. These results clearly indicate the potential of the composite-modified ta-C electrodes to measure physiologically relevant concentrations of DA at the time of release events, even in the presence of high concentrations of interferents.

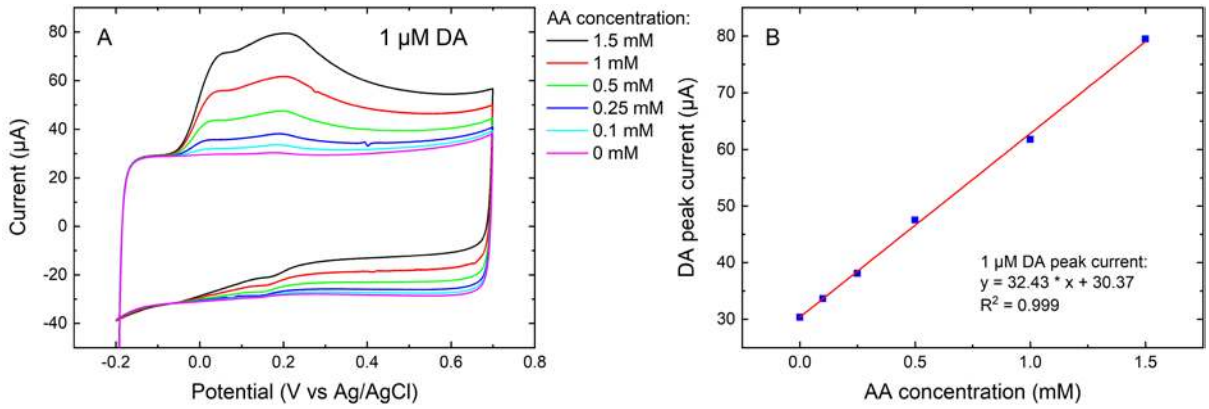

Figure 7. Cyclic voltammograms of composite-modified ta-C at 100 mV/s scan rate, showing the sensitivity towards 1 µM dopamine with varying concentrations of AA (A) and the corresponding DA peak current vs. AA concentration curve (B).

The limit of detection of the composite-modified ta-C electrode was calculated using the equation LOD = 3.3 × σ/S (where σ is the standard deviation of the blank CVs (µA) and S the slope of the calibration curve (µA/µM)). The LOD of DA in PBS and in interferent solution was 65 nM and 107 nM, respectively, in the linear range of 0.05 – 100 µM. Despite the high capacitive background current (double layer capacitance = 5.847 ± 0.163 mF/cm2, see

supplementary Figure S6), the composite material shows a high selectivity as well as physiologically relevant LOD for dopamine.

Table 1. A non-exhaustive list of publications where DA limit of detection (LOD) is calculated using CV measurements in an interferent solution containing UA and AA.

Electrode material	Interferents	Linear range (µM)	LOD in interferent solution (nM)	Scan rate (mV/s)	Reference
Pt/CNS	10 µM UA, 100 µM AA	0.8 – 2	120	100	[25]
GCE / MWCNT / PDOP / Pt NPs	0 – 60 µM UA, 0 – 4 mM AA	30 – 120	8800	50	[48]
N_MWCNT/Au NPs	100 µM UA, 500 µM AA	12 – 322	300	20	[49]
MWCNT/SNFC/Nafion modified ta-C electrode	500 µM UA, 1 mM AA	0.05 – 100	107	100	This work

Electrode explanations: Pt – platinum, CNS – carbon nanosheets, GCE – glassy carbon electrode, PDOP – polydopamine, NPs – Nanoparticles, Au – gold, N_MWCNT – nitrogen-doped MWCNTs.

A non-exhaustive list of publications where the limit of detection for dopamine was calculated using CV measurements made in an interferent solution containing AA and UA is given in Table 1. The more commonly used DPV measurements for determination of LOD in interferent solutions have not been included. Wang *et al.*[25] demonstrated a selective DA sensor using carbon nanosheets modified platinum (Pt/CNS) electrodes in 100 mV/s CV measurements, however the concentrations of interferents used were less than that demonstrated in this work. Moreover, a larger linear range has been demonstrated in the current work. The as-measured CVs in the interferent solution (Figure 6B) demonstrate the ability of the proposed sensor to selectively detect ~500 nM DA in physiologically relevant

concentrations of UA and AA even in relatively fast 100 mV/s CV measurements. To the best of the authors' knowledge, this has been demonstrated for the first time in the current work.

4. CONCLUSIONS

We have demonstrated a composite made of commercial multi-walled carbon nanotubes dispersed in a mixture of highly sulfated nanofibrillar cellulose (SNFC) and Nafion® as a modification for tetrahedral amorphous carbon electrodes. The composite-modified ta-C electrodes exhibit high sensitivity and selectivity towards dopamine in the presence of physiologically relevant concentrations of ascorbic acid and uric acid interferents in cyclic voltammetry measurements. The highly negatively charged SNFC enables the dispersion of a high concentration of MWCNTs, twice the dry weight of cellulose in the composite, while Nafion serves as a binder between the composite membrane and the hydrophobic ta-C substrate. Further, the high density of negative functional groups present in both the sulfated nanocellulose fibrils and Nafion ionomers enhance the selectivity of the composite towards the cationic dopamine molecules. The proposed sensor can selectively detect nanomolar concentration of DA in 100 mV/s scan rate CV measurements, in the presence of 1 mM AA and 0.5 mM UA. These results demonstrate hybrid nanocellulose-based composites as potential electrode materials with tailored charge transport for selective electrochemical detection of biomolecules.

ASSOCIATED CONTENT

Supporting Information

Photographs of MWCNT/SNFC, MWCNT/Nafion and composite (MWCNT/SNFC/Nafion) modified ta-C electrodes in dry state (A) and after 15 minutes of soaking in PBS solution (B). Cyclic voltammograms of MWCNT/SNFC, MWCNT/Nafion and (MWCNT/SNFC/Nafion) composite-modified ta-C electrodes in PBS solution containing 50 µM DA with 0.5 mM UA and 1 mM AA at a scan rate of 100 mV/s. EDS analysis at low magnification using scanning electron microscope. The effect of scan rates on the cyclic voltammograms of AA, UA and DA individually and in same solution. Linearization of anodic peak currents of AA and UA versus square root of scan rate. Cyclic voltammograms of composite-modified electrode in blank PBS.

AUTHOR INFORMATION

Corresponding Author

*Tel.: +358505138355. E-mail: vasuki.durairaj@aalto.fi (Vasuki Durairaj)

ORCID

Vasuki Durairaj: 0000-0001-9632-1703

Notes

The authors declare no competing financial interest.

ACKNOWLEDGMENTS

This work was supported by Business Finland funding (previously Tekes- the Finnish Funding Agency for Technology and Innovation) under the projects FEDOC (grant number 211637) and PrepIDEA (grant number 211755). The authors acknowledge the provision of facilities by Aalto University Bioeconomy and OtaNano – Nanomicroscopy Center (Aalto-NMC) and RawMatters reseach infrastructure (RAMI). The Academy of Finland Center of

Excellence on Molecular Engineering of Biosynthetic Hybrid Materials Research (HYBER) is also acknowledged for supporting this work.

REFERENCES

(1) Xu, S.; Flynn, D.; Tay, B. K.; Prawer, S.; Nugent, K. W.; Silva, S. R. P.; Lifshitz, Y.; Milne, W. I. Mechanical Properties and Raman Spectra of Tetrahedral Amorphous Carbon Films with High Sp3 Fraction Deposited Using a Filtered Cathodic Arc. *Philos. Mag. B* **1997**, *76*, 351–361.

(2) Yoo, K.; Miller, B.; Kalish, R.; Shi, X. Electrodes of Nitrogen-Incorporated Tetrahedral Amorphous Carbon. *Electrochem. Solid-State Lett.* **1999**, *2*, 233–235.

(3) Kaivosoja, E.; Suvanto, P.; Aura, S. Cell Adhesion and Osteogenic Differentiation on Three-Dimensional Pillar Surfaces. *J. Biomed. Mater. Res. A* **2013**, *101A*, 842–852.

(4) Tujunen, N.; Kaivosoja, E.; Protopopova, V.; Valle-Delgado, J. J.; Österberg, M.; Koskinen, J.; Laurila, T. Electrochemical Detection of Hydrogen Peroxide on Platinum-Containing Tetrahedral Amorphous Carbon Sensors and Evaluation of Their Biofouling Properties. *Mater. Sci. Eng. C* **2015**, *55*, 70–78.

(5) Laurila, T.; Protopopova, V.; Rhode, S.; Sainio, S.; Palomäki, T.; Moram, M.; Feliu, J. M.; Koskinen, J. New Electrochemically Improved Tetrahedral Amorphous Carbon Films for Biological Applications. *Diam. Relat. Mater.* **2014**, *49*, 62–71.

(6) Protopopova, V.; Iyer, A.; Wester, N.; Kondrateva, A.; Sainio, S.; Palomäki, T.; Laurila, T.; Mishin, M.; Koskinen, J. Ultrathin Undoped Tetrahedral Amorphous Carbon Films: The Role of the Underlying Titanium Layer on the Electronic Structure. *Diam. Relat. Mater.* **2015**, *57*, 43–52.

(7) Sainio, S.; Nordlund, D.; Caro, M. A.; Gandhiraman, R.; Koehne, J.; Wester, N.; Koskinen, J.; Meyyappan, M.; Laurila, T. Correlation between Sp 3 -to-Sp 2 Ratio and Surface Oxygen Functionalities in Tetrahedral Amorphous Carbon (Ta-C) Thin Film Electrodes and Implications of Their Electrochemical Properties. *J. Phys. Chem. C* **2016**, *120*, 8298–8304.

(8) Palomäki, T.; Wester, N.; Caro, M. A.; Sainio, S.; Protopopova, V.; Koskinen, J.; Laurila, T. Electron Transport Determines the Electrochemical Properties of Tetrahedral Amorphous Carbon (Ta-C) Thin Films. *Electrochim. Acta* **2017**, *225*, 1–10.

(9) Wester, N.; Etula, J.; Lilius, T.; Sainio, S.; Laurila, T.; Koskinen, J. Selective Detection of Morphine in the Presence of Paracetamol with Anodically Pretreated Dual Layer Ti/Tetrahedral Amorphous Carbon Electrodes. *Electrochem. commun.* **2018**, *86*, 166–170.

(10) Etula, J.; Wester, N.; Sainio, S.; Laurila, T.; Koskinen, J. Characterization and Electrochemical Properties of Iron-Doped Tetrahedral Amorphous Carbon (Ta-C) Thin Films. *RSC Adv.* **2018**, *8*, 26356–26363.

(11) Wester, N.; Sainio, S.; Palomäki, T.; Nordlund, D.; Singh, V. K.; Johansson, L. S.; Koskinen, J.; Laurila, T. Partially Reduced Graphene Oxide Modified Tetrahedral Amorphous Carbon Thin-Film Electrodes as a Platform for Nanomolar Detection of Dopamine. *J. Phys. Chem. C* **2017**, *121*, 8153–8164.

(12) Peltola, E.; Wester, N.; Holt, K. B.; Johansson, L. S.; Koskinen, J.; Myllymäki, V.; Laurila, T. Nanodiamonds on Tetrahedral Amorphous Carbon Significantly Enhance Dopamine Detection and Cell Viability. *Biosens. Bioelectron.* **2017**, *88*, 273–282.

(13) Palomäki, T.; Peltola, E.; Sainio, S.; Wester, N.; Pitkänen, O.; Kordas, K.; Koskinen, J.;

Laurila, T. Unmodified and Multi-Walled Carbon Nanotube Modified Tetrahedral Amorphous Carbon (Ta-C) Films as in Vivo Sensor Materials for Sensitive and Selective Detection of Dopamine. *Biosens. Bioelectron.* **2018**, *118*, 23–30.

(14) Mynttinen, E.; Wester, N.; Lilius, T.; Kalso, E.; Koskinen, J. Simultaneous Electrochemical Detection of Tramadol and O-Desmethyltramadol with Nafion-Coated Tetrahedral Amorphous Carbon Electrode. *Electrochim. Acta* **2019**, *295*, 347–353.

(15) Sainio, S.; Palomäki, T.; Rhode, S.; Kauppila, M.; Pitkänen, O.; Selkälä, T.; Toth, G.; Moram, M.; Kordas, K.; Koskinen, J.; et al. Chemical Carbon Nanotube (CNT) Forest Grown on Diamond-like Carbon (DLC) Thin Films Significantly Improves Electrochemical Sensitivity and Selectivity towards Dopamine. *Sens. Actuators. B. Chem.* **2015**, *211*, 177–186.

(16) Laurila, T.; Sainio, S.; Caro, M. Hybrid Carbon Based Nanomaterials for Electrochemical Detection of Biomolecules. *Prog. Mater. Sci.* **2017**, *88*, 499–594.

(17) Ferapontova, E. E. Electrochemical Analysis of Dopamine : Perspectives of Specific In Vivo Detection. *Electrochim. Acta* **2017**, *245*, 664–671.

(18) Jacobs, C. B.; Ivanov, I. N.; Nguyen, M. D.; Zestos, A. G.; Venton, B. J. High Temporal Resolution Measurements of Dopamine with Carbon Nanotube Yarn Microelectrodes. *Anal. Chem.* **2014**, *86*, 5721–5727.

(19) Deiminiat, B.; Rounaghi, G. H.; Arbab-Zavar, M. H. Development of a New Electrochemical Imprinted Sensor Based on Poly-Pyrrole, Sol–Gel and Multiwall Carbon Nanotubes for Determination of Tramadol. *Sens. Actuators. B. Chem.* **2017**, *238*, 651–659.

(20) Ji, D.; Liu, Z.; Liu, L.; Low, S. S.; Lu, Y.; Yu, X.; Zhu, L.; Li, C.; Liu, Q. Smartphone-

Based Integrated Voltammetry System for Simultaneous Detection of Ascorbic Acid, Dopamine, and Uric Acid with Graphene and Gold Nanoparticles Modified Screen-Printed Electrodes. *Biosens. Bioelectron.* **2018**, *119*, 55–62.

(21) Dhanjai; Sinha, A.; Lu, X.; Wu, L.; Tan, D.; Li, Y.; Chen, J.; Jain, R. Voltammetric Sensing of Biomolecules at Carbon Based Electrode Interfaces: A Review. *TrAC - Trends Anal. Chem.* **2018**, *98*, 174–189.

(22) Wang, J.; Musameh, M.; Lin, Y. Solubilization of Carbon Nanotubes by Nafion toward the Preparation of Amperometric Biosensors. *J. Am. Chem. Soc.* **2003**, *125*, 2408–2409.

(23) Hočevar, S. B.; Wang, J.; Deo, R. P.; Musameh, M.; Ogorevc, B. Carbon Nanotube Modified Microelectrode for Enhanced Voltammetric Detection of Dopamine in the Presence of Ascorbate. *Electroanalysis* **2005**, *17*, 417–422.

(24) Wang, H. S.; Li, T. H.; Jia, W. L.; Xu, H. Y. Highly Selective and Sensitive Determination of Dopamine Using a Nafion/Carbon Nanotubes Coated Poly(3-Methylthiophene) Modified Electrode. *Biosens. Bioelectron.* **2006**, *22*, 664–669.

(25) Wang, Z.; Shoji, M.; Ogata, H. Facile Low-Temperature Growth of Carbon Nanosheets toward Simultaneous Determination of Dopamine, Ascorbic Acid and Uric Acid. *Analyst* **2011**, *136*, 4903–4905.

(26) Abdul Khalil, H. P. S.; Davoudpour, Y.; Islam, M. N.; Mustapha, A.; Sudesh, K.; Dungani, R.; Jawaid, M. Production and Modification of Nanofibrillated Cellulose Using Various Mechanical Processes: A Review. *Carbohydr. Polym.* **2014**, *99*, 649–665.

(27) Liimatainen, H.; Visanko, M.; Sirviö, J.; Hormi, O.; Niinimäki, J. Sulfonated Cellulose Nanofibrils Obtained from Wood Pulp through Regioselective Oxidative Bisulfite Pre-

Treatment. *Cellulose* **2013**, *20*, 741–749.

(28) Zhang, Y.; Nypelö, T.; Salas, C.; Arboleda, J.; Hoeger, I. C.; Rojas, O. J. Cellulose Nanofibrils. *J. Renew. Mater.* **2013**, *1*, 195–211.

(29) Bonné, M. J.; Galbraith, E.; James, T. D.; Wasbrough, M. J.; Edler, K. J.; Jenkins, A. T. A.; Helton, M.; McKee, A.; Thielemans, W.; Psillakis, E.; et al. Boronic Acid Dendrimer Receptor Modified Nanofibrillar Cellulose Membranes. *J. Mater. Chem.* **2010**, *20*, 588–594.

(30) Shariki, S.; Liew, S. Y.; Thielemans, W.; Walsh, D. A.; Cummings, C. Y.; Rassaei, L.; Wasbrough, M. J.; Edler, K. J.; Bonné, M. J.; Marken, F. Tuning Percolation Speed in Layer-by-Layer Assembled Polyaniline- Nanocellulose Composite Films. *J. Solid State Electrochem.* **2011**, *15*, 2675–2681.

(31) Bonné, M. J.; Edler, K. J.; Buchanan, J. G.; Wolverson, D.; Psillakis, E.; Helton, M.; Thielemans, W.; Marken, F. Thin-Film Modified Electrodes with Reconstituted Cellulose-PDDAC Films for the Accumulation and Detection of Triclosan. *J. Phys. Chem. C* **2008**, *112*, 2660–2666.

(32) Hamedi, M. M.; Hajian, A.; Fall, A. B.; Hkansson, K.; Salajkova, M.; Lundell, F.; Wgberg, L.; Berglund, L. A. Highly Conducting, Strong Nanocomposites Based on Nanocellulose-Assisted Aqueous Dispersions of Single-Wall Carbon Nanotubes. *ACS Nano* **2014**, *8*, 2467–2476.

(33) Li, Y.; Zhu, H.; Shen, F.; Wan, J.; Lacey, S.; Fang, Z.; Dai, H.; Hu, L. Nanocellulose as Green Dispersant for Two-Dimensional Energy Materials. *Nano Energy* **2015**, *13*, 346–354.

(34) Hajian, A.; Lindström, S. B.; Pettersson, T.; Hamedi, M. M.; Wågberg, L.

Understanding the Dispersive Action of Nanocellulose for Carbon Nanomaterials. *Nano Lett.* **2017**, *17*, 1439–1447.

(35) Xing, J.; Tao, P.; Wu, Z.; Xing, C.; Liao, X.; Nie, S. Nanocellulose-Graphene Composites: A Promising Nanomaterial for Flexible Supercapacitors. *Carbohydr. Polym.* **2019**, *207*, 447–459.

(36) Nguyen, H. K.; Bae, J.; Hur, J.; Park, S. J.; Park, M. S.; Kim, I. T. Tailoring of Aqueous-Based Carbon Nanotube – Nanocellulose Films as Self-Standing Flexible Anodes for Lithium-Ion Storage. *Nanomaterials* **2019**, *9*, 655.

(37) Koga, H.; Saito, T.; Kitaoka, T.; Nogi, M.; Suganuma, K.; Isogai, A. Transparent, Conductive, and Printable Composites Consisting of TEMPO-Oxidized Nanocellulose and Carbon Nanotube. *Biomacromolecules* **2013**, *14*, 1160–1165.

(38) Shahrokhian, S.; Naderi, L.; Ghalkhani, M. Nanocellulose/Carbon Nanoparticles Nanocomposite Film Modified Electrode for Durable and Sensitive Electrochemical Determination of Metoclopramide. *Electroanalysis* **2015**, *27*, 2637–2644.

(39) Muguruma, H.; Inoue, Y.; Inoue, H.; Ohsawa, T. Electrochemical Study of Dopamine at Electrode Fabricated by Cellulose-Assisted Aqueous Dispersion of Long-Length Carbon Nanotube. *J. Phys. Chem. C* **2016**, *120*, 12284–12292.

(40) Shalauddin, M.; Akhter, S.; Basirun, W. J.; Bagheri, S.; Anuar, N. S.; Johan, M. R. Hybrid Nanocellulose/f-MWCNTs Nanocomposite for the Electrochemical Sensing of Diclofenac Sodium in Pharmaceutical Drugs and Biological Fluids. *Electrochim. Acta* **2019**, *304*, 323–333.

(41) Gu, J.; Catchmark, J. M.; Kaiser, E. Q.; Archibald, D. D. Quantification of Cellulose Nanowhiskers Sulfate Esterification Levels. *Carbohydr. Polym.* **2013**, *92*, 1809–1816.

(42) Ramaswamy, N.; Hakim, N.; Mukerjee, S. Degradation Mechanism Study of Perfluorinated Proton Exchange Membrane under Fuel Cell Operating Conditions. *Electrochim. Acta* **2008**, *53*, 3279–3295.

(43) Chikvaidze, G.; Gabrusenoks, J.; Kleperis, J.; Vaivars, G. Application of Micro Raman Spectroscopy to Industrial FC Membranes. *J. Phys. Conf. Ser.* **2007**, *93*, 012026.

(44) Gremlich, H.-U.; Yan, B. *Infrared and Raman Spectroscopy of Biological Materials*; CRC Press: Boca Raton, 2000.

(45) Okpalugo, T. I. T.; Papakonstantinou, P.; Murphy, H.; McLaughlin, J.; Brown, N. M. D. Oxidative Functionalization of Carbon Nanotubes in Atmospheric Pressure Filamentary Dielectric Barrier Discharge (APDBD). *Carbon N. Y.* **2005**, *43*, 2951–2959.

(46) Thielemans, W.; Warbey, C. R.; Walsh, D. A. Permselective Nanostructured Membranes Based on Cellulose Nanowhiskers. *Green Chem.* **2009**, *11*, 531–537.

(47) Palomäki, T.; Chumillas, S.; Sainio, S.; Protopopova, V.; Kauppila, M.; Koskinen, J.; Climent, V.; Feliu, J. M.; Laurila, T. Electrochemical Reactions of Catechol, Methylcatechol and Dopamine at Tetrahedral Amorphous Carbon (Ta-C) Thin Film Electrodes. *Diam. Relat. Mater.* **2015**, *59*, 30–39.

(48) Lin, M.; Huang, H.; Liu, Y.; Liang, C.; Fei, S.; Chen, X.; Ni, C. High Loading of Uniformly Dispersed Pt Nanoparticles on Polydopamine Coated Carbon Nanotubes and Its Application in Simultaneous Determination of Dopamine and Uric Acid. *Nanotechnology* **2013**, *24*, 065501.

(49) Tsierkezos, N. G.; Othman, S. H.; Ritter, U.; Hafermann, L.; Knauer, A.; Köhler, J. M.; Downing, C.; McCarthy, E. K. Electrochemical Analysis of Ascorbic Acid, Dopamine, and Uric Acid on Nobel Metal Modified Nitrogen-Doped Carbon Nanotubes. *Sens.*

Actuators. B. Chem. **2016**, *231*, 218–229.

TOC GRAPHIC

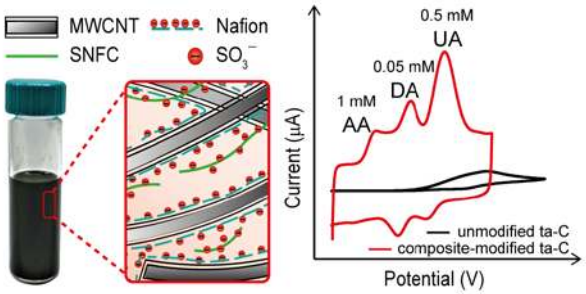
MWCNT
Nafion
SNFC
SO_3^-
0.5 mM
UA
0.05 mM
DA
1 mM
AA
Current (μA)
Potential (V)
unmodified ta-C
composite-modified ta-C